

Supporting information for

“Extremely selective detection of ppb-levels indoor xylene using CoCr₂O₄ hollow spheres activated by Pt doping”

Kun Ho Lee,^a Bo-Young Kim,^a Ji-Wook Yoon,^{a,*} and Jong-Heun Lee^{a,*}

^aDepartment of Materials Science and Engineering, Korea University, Seoul 02841, Korea

* Authors to whom correspondence should be addressed

Ji-Wook Yoon: uhpupu@korea.ac.kr, Tel: +82-23290-3710

Jong-Heun Lee: jongheun@korea.ac.kr, Tel: +82-2-3290-3282

Experimental Section

Preparation of pure, Pt-, Au-, and Pd-CoCr₂O₄ hollow spheres:

Pure CoCr₂O₄ hollow spheres were prepared by one-pot ultrasonic spray pyrolysis of an aqueous solution (200 mL) containing Cobalt (II) nitrate hexahydrate (0.375 g, Co(NO₃)₂·6H₂O, >98%, Sigma-Aldrich, UK), Chromium (III) nitrate nonahydrate (1.020 g, Cr(NO₃)₃·9H₂O, >99.99%, Sigma-Aldrich, USA), and citric acid (1.005 g, C₆H₈O₇, 99.5%, Sigma-Aldrich, Japan). The spray-pyrolysis equipment consisted of the droplet generator, tubular reactor, and powder-collecting chamber. The droplets of the solution were generated by five ultrasonic transducers (frequency = 1.67 MHz), which were carried into a tubular quartz reactor (temperature = 600 °C, length = 1200 mm, diameter = 50 mm) by air at a flow rate of 10 L/min. A Teflon bag filter was used to collect the precursor powders. The CoCr₂O₄ hollow spheres were prepared by annealing the precursor powders at 700 °C for 2 h in air.

The Pt-, Au-, and Pd-CoCr₂O₄ hollow spheres were synthesized by the same procedure after the addition of chloroplatinic acid solution, 8 wt% in H₂O (0.015 mL, H₂PtCl₆, Sigma-Aldrich, USA), palladium nitrate hydrate (0.0014 g, Pd(NO₃)₂·xH₂O, Sigma-Aldrich, USA), and gold chloride trihydrate (0.0012 g, HAuCl₄·3H₂O, Sigma-Aldrich, USA) in the solution, respectively. The ratio between Pt, Au, and Au and Co and Cr ([Pt, Au, or Au]/[Co + 2Cr]) were fixed to 0.3 wt%. The Pt-, Au-, and Pd-CoCr₂O₄ spheres were prepared by the heat-treatment of the precursor powders at 700 °C for 2 h in air.

Characterization:

The morphologies of the sensing materials were investigated by using field emission scanning electron microscopy (SEM, SU-70, Hitachi Co., Ltd., Japan) and high-resolution transmission electron microscopy (HR-TEM, JEM-2100F, JEOL, Japan). The phases and crystal structures were analyzed via X-ray diffractometry (XRD, D/MAX-2500, Rigaku, Japan) with $\text{CuK}\alpha$ radiation ($\lambda = 1.5418 \text{ \AA}$). The chemical states of each sample were observed using X-ray photoelectron spectroscopy (XPS, MultiLab 2000, Thermo Scientific, USA). Inductively coupled plasma-atomic emission spectroscopy (ICP-AES, Optima 4300 DV, Perkin Elmer Instruments, USA) was used to determine the concentration of Pt, Au, and Pd in the CoCr_2O_4 hollow spheres. The specific surface areas of the spheres were determined from a Brunauer–Emmett–Teller (BET) analysis of nitrogen-adsorption measurements (BET, TriStar 3000, Micromeritics, Norcross, MN, USA).

Gas sensing characteristics:

The pure, Pt-, Au-, and Pd- CoCr_2O_4 hollow spheres were made in a slurry form and drop-coated on an alumina substrate (size: $1.5 \times 1.5 \text{ mm}^2$, thickness: 0.25 mm) with two Au electrodes on the top (spacing: 200 μm) and a micro-heater on the bottom. The sensors were heat-treated at 450°C for 2 h to remove residual water-related species (e.g., hydroxyl groups) and to stabilize the sensors. For the measurement, the sensors were contained in a specially designed, low volume (1.5 cm^3) quartz tube to minimize delay in changing the atmosphere controlled by a four-way valve. The flow rates for both dry air and analytic gases were $200 \text{ cm}^3 \text{ min}^{-1}$. The concentration of analytic gases was controlled by changing the mixing ratio between 5 ppm of *p*-xylene, toluene, ethanol, trimethylamine, ammonia, formaldehyde, benzene, and carbon monoxide (in air balance) and synthetic dry air. The direct-current 2-probe resistance of the sensor was measured using an electrometer (6487 Picoammeter, Keithley, Tecktronic Inc., USA) interfaced with a computer. The gas responses ($S = R_g R_a^{-1}$; R_g : resistance in analytic gas, R_a : resistance in air) of the sensors were evaluated in the range of 250 – 350°C.

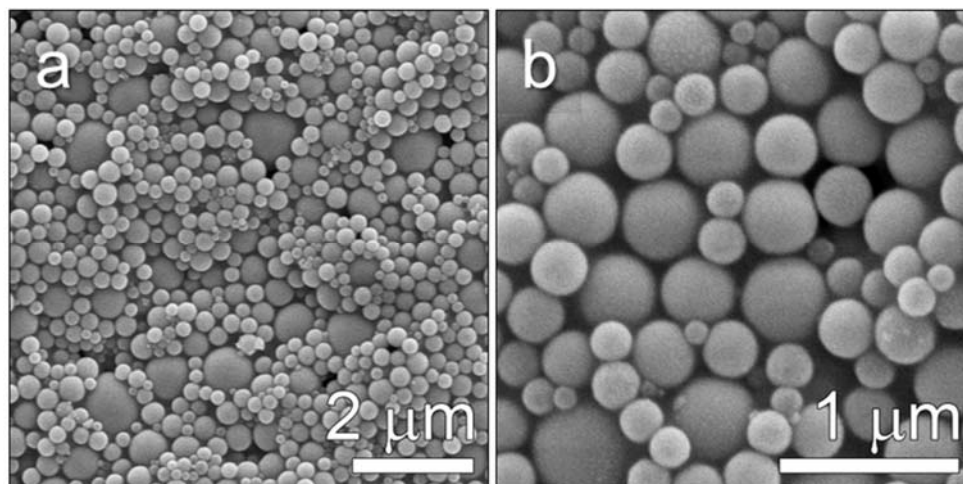


Figure S1. (a) Low and (b) high magnification SEM images for Pt-CoCr precursor spheres after spray pyrolysis.

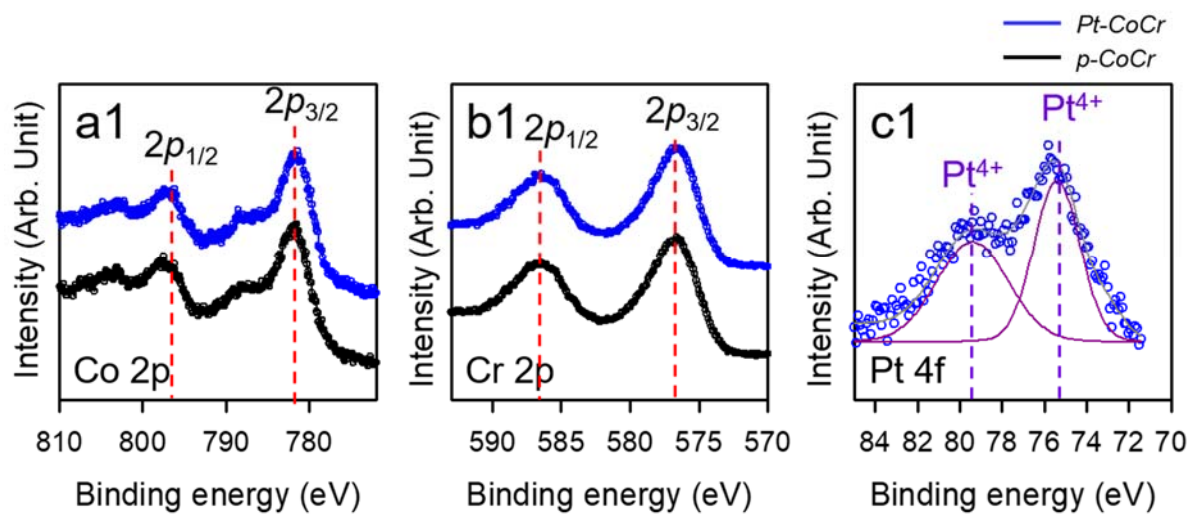


Figure S2. XPS spectra for (a) Co 2p, (b) Cr 2p, and (c) Pt 4f of Pt-CoCr (blue) and p-CoCr (black).

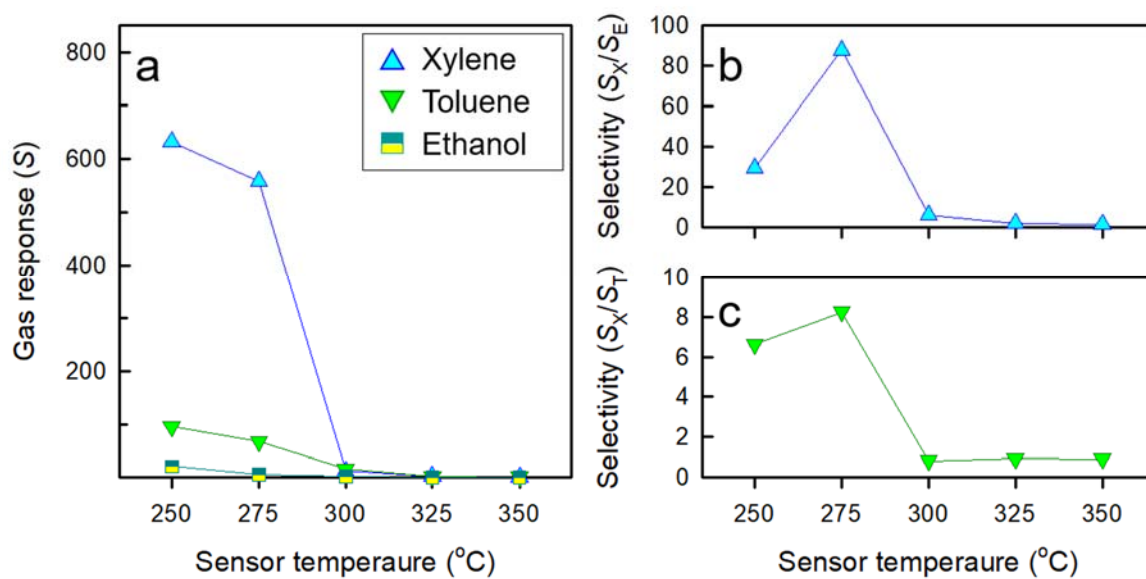


Figure S3. (a) Gas responses of Pt-CoCr to 5 ppm of xylene, toluene, and ethanol at 250 – 350 °C. (b, c) Xylene selectivity (S_X/S_E or S_X/S_T) at the same temperatures.

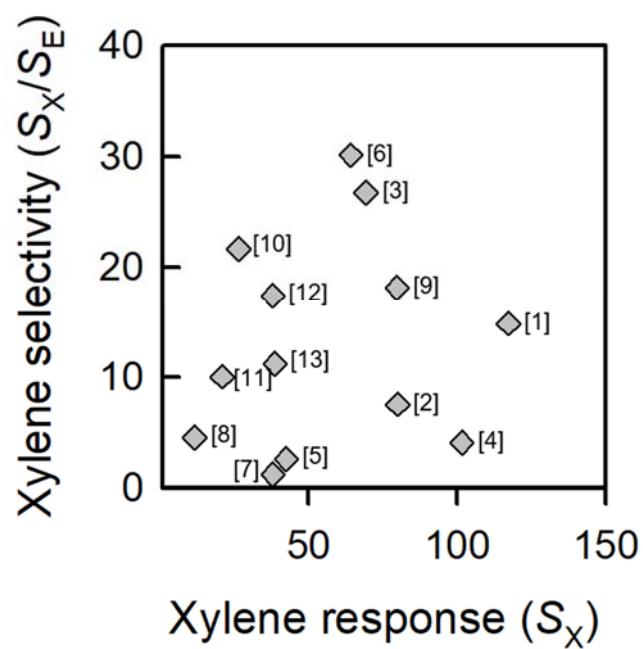


Figure S4. The xylene selectivity (S_X/S_E) and response (S_X) reported in the literature.¹⁻¹³

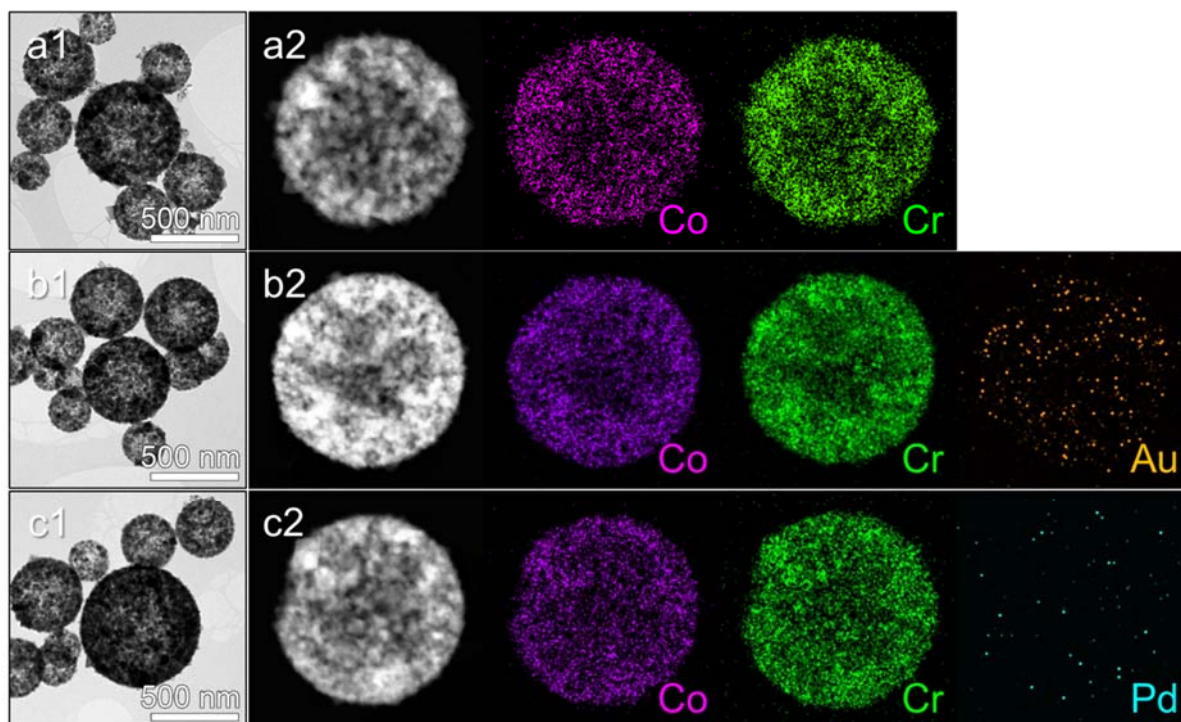


Figure S5. (a1-c1) TEM and (a2-c2) elemental-mapping images of (a) p-CoCr, (b) Au-CoCr, and (c) Pd-CoCr.

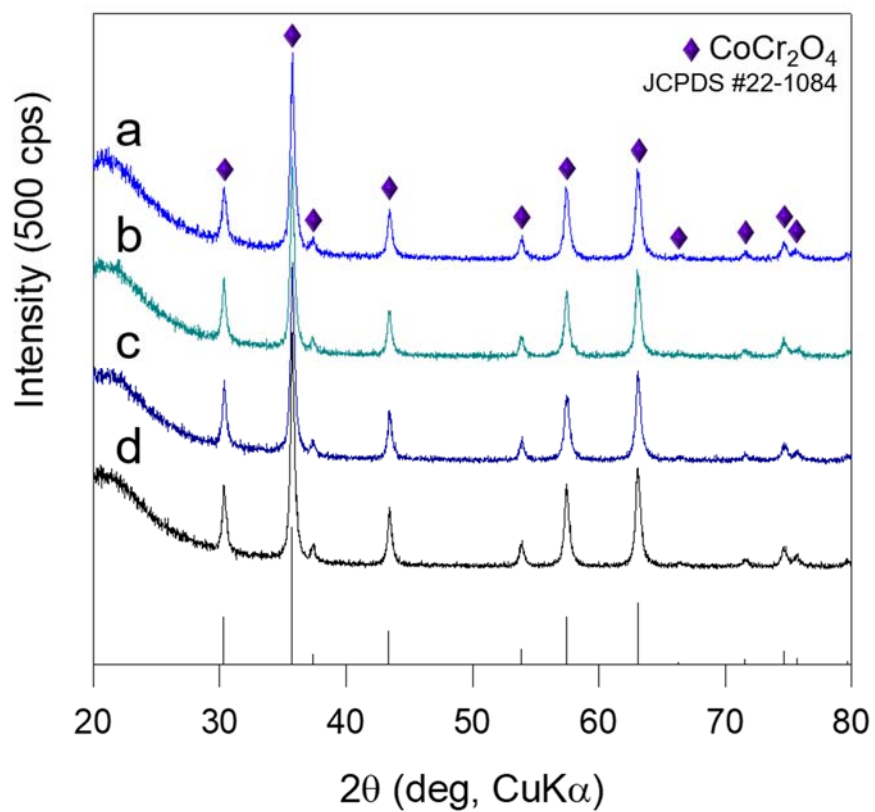


Figure S6. XRD patterns of (a) Pt-CoCr, (b) Au-CoCr, (c) Pd-CoCr, and (d) p-CoCr.

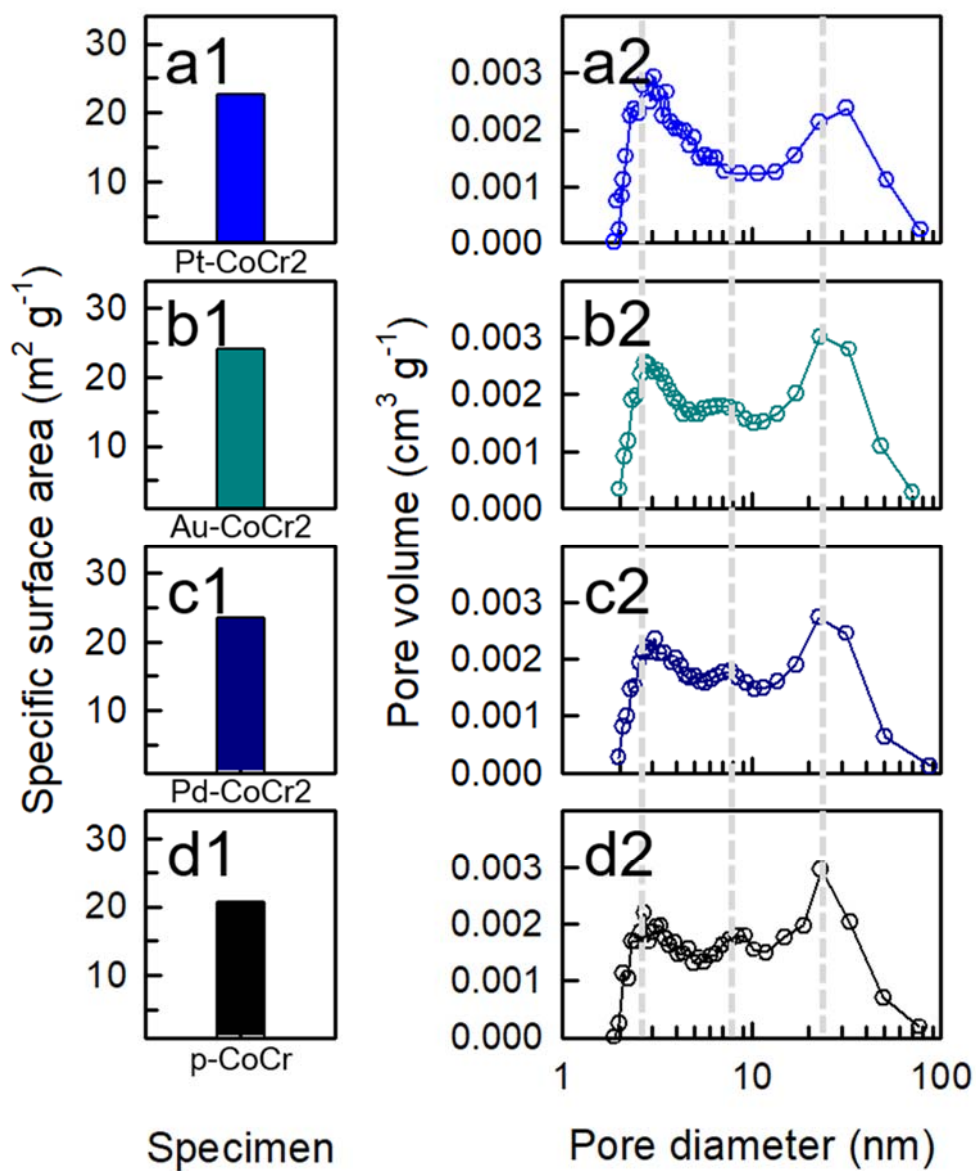


Figure S7. (a1-d1) BET specific surface areas and (a2-d2) pore size distributions of (a) Pt-CoCr, (b) Au-CoCr, (c) Pd-CoCr, and (d) p-CoCr hollow spheres.

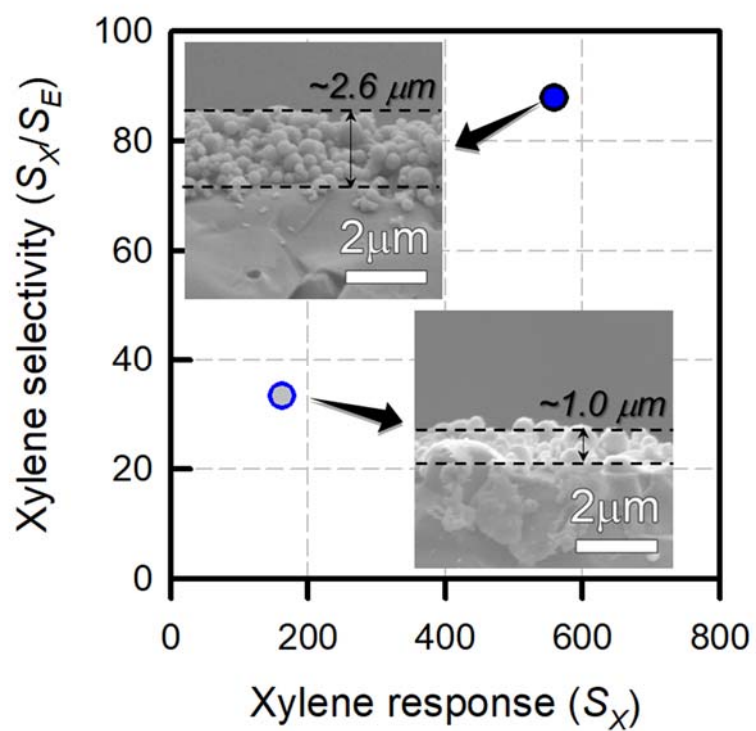


Figure S8. (a) Xylene selectivity (S_X/S_E) and (b) response (S_X) of Pt-CoCr depending on the sensing film thickness.

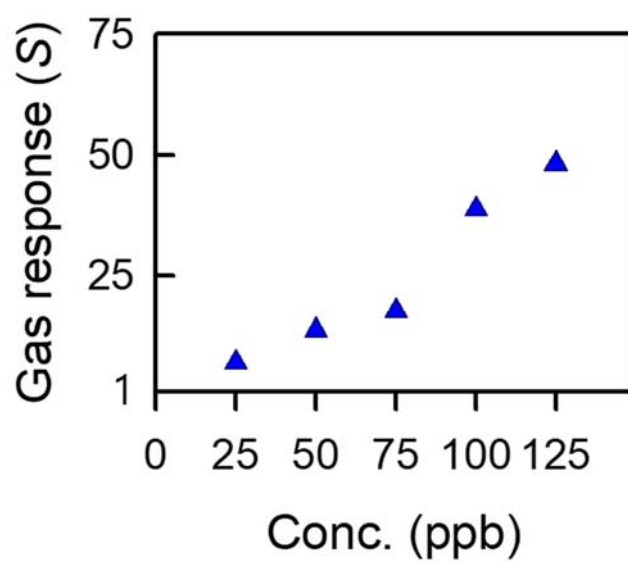


Figure S9. Gas responses of Pt-CoCr sensor to 25 – 125 ppb of xylene at 275°C under the relative humidity of 80 %.

Table S1. The values of 5 ppm xylene selectivity (S_X/S_E) and response (S_X) in the present study compared to the reported values in the literature.¹⁻¹³

No.	Sensing materials	Structure	Temp. (°C)	Response (S_X)	Selectivity (S_X/S_E)	LOD (ppm)	Ref
1	Pt-CoCr ₂ O ₄	Hollow	275	558.8	87.8	0.019	This study
2	Pd-CoCr ₂ O ₄	Hollow	275	225.8	30.7		This study
3	Au-CoCr ₂ O ₄	Hollow	275	365.5	30.9		This study
4	CoCr ₂ O ₄	Hollow	275	319.5	25.4		This study
5	CoCr ₂ O ₄ -Cr ₂ O ₃	Hollow	275	117.2	14.8	≤ 0.25	[1]
6	Co ₃ O ₄	Hollow hierarchical	225	80	7.5	≤ 0.25	[2]
7	ZnCr ₂ O ₄	Hetero nanostructure	325	69.2	26.7	≤ 0.25	[3]
8	NiMoO ₄	Hierarchical	375	101.5	4.06	0.02	[4]
9	Ni-doped ZnO	Nanowire	400	42.44	2.54	0.04	[5]
10	Pd-loaded Co ₃ O ₄	Yolk-shell	250	64.2	30.1	≤ 0.25	[6]
11	Co ₃ O ₄	Hierarchical	150	37.9	1.18	≤ 1	[7]
12	Cr-doped NiO	Hierarchical	400	11.61	4.48	≤ 0,25	[8]
13	Pd-loaded Co ₃ O ₄	Hierarchical	300	79.7	18.1	0.2	[9]
14	Au-loaded WO ₃ ·H ₂ O	Nanocube	255	26.4	21.64	0.2	[10]
15	Cr-loaded NiO	Core-shell	220	20.9	~ 10	1	[11]
16	Co ₃ O ₄	Hierarchical nanosheet	150	37.9	17.4	≤ 1	[12]
17	Co ₃ O ₄	Flower	150	38.7	11.18	≤ 1	[13]

References

- 1 B.-Y. Kim, J.-W. Yoon, K. Lim, S. H. Park, J.-W. Yoon and J.-H. Lee, *J. Mater. Chem. C*, DOI: 10.1039/C8TC04166K.
- 2 Y.-M. Jo, T.-H. Kim, C.-S. Lee, K. Lim, C. W. Na, F. Abdel-Hady, A. A. Wazzan and J. H. Lee, *ACS Appl. Mater. Interfaces*, 2018, **10**, 8860.
- 3 J.-H. Kim, H.-M. Jeong, C. W. Na, J.-W. Yoon, F. Abdel-Hady, A. A. Wazzan and J. H. Lee, *Sens. Actuators B*, 2016, **235**, 498.
- 4 B.-Y. Kim, J. H. Ahn, J.-W. Yoon, C.-S. Lee, Y. C. Kang, F. Abdel-Hady, A. A. Wazzan and J.-H. Lee, *ACS Appl. Mater. Interfaces*, 2016, **8**, 34603.
- 5 H.-S. Woo, C.-H. Kwak, J.-H. Chung and J.-H. Lee, *Sens. Actuators B*, 2015, **216**, 358.
- 6 J.-W. Yoon, Y. J. Hong, G. D. Park, S.-J. Hwang, F. Abdel-Hady, A. A. Wazzan, Y. C. Kang and J.-H. Lee, *ACS Appl. Mater. Interfaces*, 2015, **7**, 7717.
- 7 K. Xu, J. Zou, S. Tian, Y. Yong, F. Zeng, T. Yu, Y. Zhang, X. Jie and C. Yuan, *Sens. Actuators B*, 2017, **246**, 68.
- 8 H.-J. Kim, J.-W. Yoon, K.-I. Choi, H. W. Jang, A. Umar and J.-H. Lee, *Nanoscale*, 2013, **5**, 7066.
- 9 S.-J. Hwang, K.-I. Choi, J.-W. Yoon, Y. C. Kang and J.-H. Lee, *Chem. Eur. J.*, 2015, **21**, 5872.
- 10 F. Li, S. Guo, J. Shen, L. Shen, D. Sun, B. Wang, Y. Chen and S. Ruan, *Sens. Actuators B*, 2017, **238**, 364.
- 11 J. Cao, Z. Wang, R. Wang and T. Zhang, *CrystEngComm*, 2014, **16**, 7731.
- 12 K. Xu, J. Zou, S. Tian, Y. Yang, F. Zeng, T. Yu, Y. Zhang, X. Jie and C. Yuan, *Sens. Actuators B*, 2017, **246**, 68.

13 K. Xu, L. Yang, J. Zou, Y. Yang, Q. Li, Y. Qu, J. Ye and C. Yuan, *J. Alloys Compd.* 2017, **246**,

68.